J. Magn. Soc. Jpn., **49**, 13-16 (2025) <Letter>

Spin wave nonreciprocity due to asymmetry of propagation length

Haruka Komiyama[1], Ryusuke Hisatomi[1,2,3], Kotaro Taga[1], Hiroki Matsumoto[1], Hideki Narita[1,3], Shutaro Karube[1,2,3], Yoichi Shiota[1,2], and Teruo Ono[1,2]

[1]Institute for Chemical Research (ICR), Kyoto Univ., *Gokasho, Uji, Kyoto 611-0011, Japan*
[2]Center for Spintronics Research Network (CSRN), Kyoto Univ., *Gokasho, Uji, Kyoto 611-0011, Japan*
[3]PRESTO, Japan Science and Technology Agency, *Kawaguchi-shi, Saitama 332-0012, Japan*

Nonreciprocity of spin waves, which means the difference in amplitude depending on the direction of propagation, provides functionality to spin wave-based devices. One of the known origins of spin wave nonreciprocity is the asymmetry of the excitation efficiency due to the asymmetry of the out-of-plane microwave magnetic field generated by an antenna. We investigate the magnetic field angle dependence of spin wave nonreciprocity. We find that this nonreciprocity is due to the asymmetry of the propagation length in addition to the asymmetry of the excitation efficiency.

Keywords: nonreciprocity, spin wave, magneto-optical imaging, magnetic thin film, propagation length, dissipation

1. Introduction

Spin waves in a magnetic thin film on a substrate are expected to be next-generation information carriers because they can transmit information with low power consumption without charge transfer. Furthermore, spin waves have nonreciprocity, meaning their behavior depends on the propagation direction. Understanding the nonreciprocity of spin waves is directly linked to constructing magnonic logic circuits [1)-4)].

In a magnetic thin film thinner enough than the wavelength, a microstrip antenna's spin wave excitation efficiency depends on the propagation direction due to the asymmetry of the out-of-plane microwave magnetic field, creating the amplitude nonreciprocity. The effect is theoretically suggested to depend on the relative angle between the direction of the propagation and the magnetic field. Previous researches investigated nonreciprocity when the relative angles are 90 degrees and 0 degrees, finding that the behavior was consistent with the theoretical suggestions [5),6)].

In this study, we investigate the nonreciprocity at intermediate angles and find that it reaches a local maximum at two specific angle regions. The above mechanism cannot explain all of this angle dependence, implying that another mechanism causes the nonreciprocity. By optical imaging of the spin waves, we find that the spin wave propagation length is asymmetric. Our results suggest that the nonreciprocity of the spin waves is characterized by both the asymmetry of the excitation efficiency and the propagation length.

2. Experiments and Results

2.1 Device preparation

Figure 1(a) shows a schematic illustration of the device and the electrical transmission measurement system. We first deposit 100 μm × 100 μm-sized CoFeB (50) and Ta (2) on a thermally oxidized Si substrate using magnetron sputtering. The numbers in parentheses indicate the thicknesses of the films, and the unit is nm. After that, we deposit SiO_2 (60) as an insulating layer and then deposit two 0.5 μm -wide, 130 μm -long microstrip antennas for exciting and detecting spin waves. The antennas are made of Ti (5)/ Cu (150)/ Au (20) and are 10 μm apart.

2.2 Electrical measurements

To investigate the nonreciprocity of spin waves between the two antennas, we obtain the transmission coefficients S_{12} and S_{21} using a vector network analyzer (VNA) under the conditions shown in Fig. 1(a) where an in-plane magnetic field H_{DC} is applied in the direction of the angle θ from the x-axis. To avoid additional dissipation due to the nonlinearity of the spin waves, we set the microwave power input from the VNA to the antenna to -5 dBm. The frequency range for the transmission measurements is set to 3 to 20 GHz in 11.5 MHz steps, and the IF bandwidth is set to 10 kHz. The in-plane magnetic field $\mu_0 H_{\mathrm{DC}}$ is set in the range from 200 mT to 0 mT in 10 mT steps, and the magnetic field angle θ is set in the range from 0 to 90 degrees in 5 degrees steps. Here, μ_0 is the vacuum permeability. The obtained transmission spectrum is usually a superposition of the electromagnetic wave signal (i.e., cross-talk) and the propagating spin wave signal. To remove the cross-talk signal, we use the spectrum at 250 mT as a reference, which contains only the cross-talk because the resonance frequencies of the spin waves excited by the antenna are outside the measurement frequency range. We obtain the spectrum of the spin waves by subtracting the reference spectrum from all the spectra at each magnetic field angle θ.

Figure 1(b) shows the amplitude of the spin wave transmission spectrum measured at $\theta =$ 90 degrees and $\mu_0 H_{\mathrm{DC}} = 50$ mT, for example. The gray dotted and solid lines represent the frequencies of spin waves with wavenumbers of 0 and 1 $\mu\mathrm{m}^{-1}$, respectively, calculated

Corresponding author: H. Komiyama
(e-mail: komiyama.haruka.64v@st.kyoto-u.ac.jp).

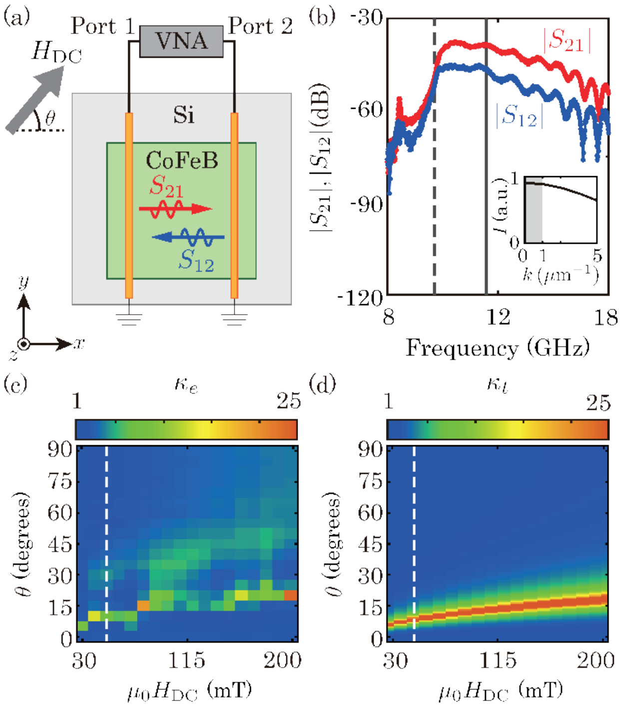

Fig. 1 (a) Experimental setup and device for observing nonreciprocity of spin waves by electrical transmission measurements. (b) Microwave transmission spectra under external magnetic field $\mu_0 H_{DC} = 50$ mT and angle $\theta = 90$ degrees. Inset shows FFT intensity I of antenna. (c)(d) Color maps of nonreciprocity of spin waves from (c) experiment κ_e and (d) theoretical model κ_t.

from the known dispersion relation of the spin waves [7]. The result in Fig. 1(b) reflects the fact that the antenna of this device can efficiently excite and detect the spin waves with the wavenumbers from 0 to 1 μm^{-1}, as predicted from the Fourier transform of the antenna shape shown in the inset of Fig. 1(b). Furthermore, the difference in the transmission amplitudes of $|S_{21}|$ and $|S_{12}|$ represents nonreciprocity. We confirm that the transmission signal of the spin waves with the wavenumbers from 0 to 1 μm^{-1} is dominant under other magnetic field conditions.

To discuss the magnetic field angle θ and magnitude H_{DC} dependences of the nonreciprocity, we define the nonreciprocity evaluated from the experiment as $\kappa_e(\theta, H_{DC}) = \sum_{\omega_a(|k|=0)}^{\omega_a(|k|=1\,\mu m^{-1})} |S_{21}| / \sum_{\omega_a(|k|=0)}^{\omega_a(|k|=1\,\mu m^{-1})} |S_{12}|$. Here, we take the sum of the transmission amplitude in the frequency range of the spin waves with the wavenumbers $|k|$ of 0 to 1 μm^{-1} for each θ and H_{DC}. Figure 1(c) shows the nonreciprocity κ_e as a function of the magnetic field magnitude $\mu_0 H_{DC}$ and angle θ. We omit the data below $\mu_0 H_{DC} = 20$ mT, where the magnetic thin film's magnetic structure is multi-domain. Figure 1(c) shows the two-angle region where the nonreciprocity reaches the local maximum at each magnetic field magnitude: around 10 to 20 degrees and 30 to 60 degrees.

To study the origin of the nonreciprocity in the experiment, we calculate the nonreciprocity κ_t derived from the asymmetries of spin wave excitation efficiency by the antenna depending on the propagation direction, which is demonstrated in the previous studies [5),6)], and compare it with Fig. 1(c). Based on the previous studies, the theoretical model $\kappa_t(\theta, H_{DC})$ can be written as

$$\kappa_t(\theta, H_{DC}) = \frac{\sum|S_{21}|}{\sum|S_{12}|} = \left(\frac{\sum_{\omega_a(|k|=0)}^{\omega_a(|k|=1\,\mu m^{-1})} \omega_M \omega_a \sin\theta + \{\omega_a^2 - \omega_H^2\}}{\sum_{\omega_a(|k|=0)}^{\omega_a(|k|=1\,\mu m^{-1})} \omega_M \omega_a \sin\theta - \{\omega_a^2 - \omega_H^2\}} \right), \quad (1)$$

where $\omega_M = \gamma\mu_0 M_s$ and $\omega_H = \gamma\mu_0 H_{DC}$. Here, $\gamma = 2\pi \times 30$ GHz/T and $\mu_0 M_s = 1.6$ T are the gyromagnetic ratio and saturation magnetization of CoFeB, respectively. ω_a is the resonance frequency of the spin waves [7] with the wavenumber k in the given θ and H_{DC}. The first and second terms in the numerator and denominator of Eq. (1) represent the excitation efficiency of the spin waves excited by the in-plane and out-of-plane microwave magnetic fields applied from the antenna, respectively. The signs between the first and second terms, positive and negative in the numerator and denominator, respectively, represent the difference in the sum of the spin wave excitation efficiency. Note that the $\sin\theta$ in the first terms mean that the in-plane microwave magnetic field component perpendicular to the equilibrium magnetization contributes to the spin wave excitation.

Figure 1(d) is the magnetic field magnitude and angle dependences of nonreciprocity κ_t calculated using Eq. (1). The calculation uses parameter steps of 10 mT for $\mu_0 H_{DC}$ and 0.1 degrees for θ. By comparing Figs. 1(c) and 1(d), we find that the model agrees well with the local maximum of nonreciprocity in the low-angle region, around 10 to 20 degrees. However, the model does not explain the other local maximum in the high-angle region, around 30 to 60 degrees, in Fig. 1(c). The result suggests the existence of another origin of the spin wave nonreciprocity.

Generally, the amplitude of a locally excited wave at a distance $|x|$ from the excitation source can be expressed as $Ae^{-|x|/\lambda}$, where A and λ are an amplitude at the excitation source and a propagation length, respectively. Hence, the properties of the amplitude A and the propagation length λ of the waves propagating in opposite directions determine the wave nonreciprocity. For the spin waves, the existing model κ_t in Eq. (1) only considers the asymmetry of the amplitude at the excitation source A. We hypothesize that the asymmetry of the propagation length is the origin of the local maximum of the nonreciprocity κ_e in the angle region, around 30 to 60 degrees.

The above discussion can be summarized

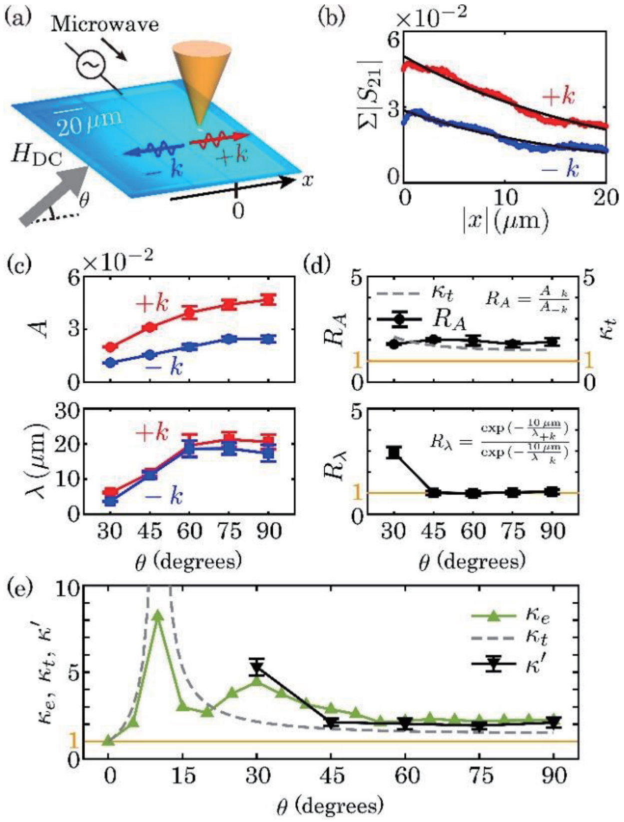

Fig. 2 (a) Optical measurement setup including microscope image of device. (b) Distance $|x|$ dependence of sum of transmission coefficient amplitudes at $\theta =$ 90 degrees, 50 mT. Solid black lines are fitting curves. (c) Angle θ dependence of amplitude $A_{\pm k}$ and propagation length $\lambda_{\pm k}$ at 50 mT. (d) Angle θ dependence of amplitude ratio R_A and propagation length ratio R_λ at $|x| = 10$ μm, using results of (c). Yellow line represents 1. (e) Angle θ dependence of nonreciprocity κ_e, κ_t, and κ' at 50 mT.

mathematically as follows. The amplitude at the excitation source and the propagation length of the spin waves propagating in the $\pm k$ directions are represented by $A_{\pm k}$ and $\lambda_{\pm k}$, respectively. The nonreciprocity κ' resulting from the asymmetries of the amplitude and the propagation length can be described by

$$\kappa' = \frac{A_{+k} e^{-\frac{|x|}{\lambda_{+k}}}}{A_{-k} e^{-\frac{|x|}{\lambda_{-k}}}} = \frac{A_{+k}}{A_{-k}} \times \frac{e^{-\frac{|x|}{\lambda_{+k}}}}{e^{-\frac{|x|}{\lambda_{-k}}}}. \quad (2)$$

It is expressed as the product of the ratio $R_A = A_{+k}/A_{-k}$ and the ratio $R_\lambda = e^{-|x|/\lambda_{+k}}/e^{-|x|/\lambda_{-k}}$. The κ_t in Eq. (1) only considers the asymmetry of the excitation efficiency of the antenna and is equal to the R_A.

2.3 Magneto-Optical Kerr effect spectroscopy

To validate our above hypothesis, we investigate R_A, R_λ, and κ' using optical imaging with the heterodyne-magneto-optical Kerr effect (MOKE) technique [8),9)]. Figure 2(a) shows the schematic illustration of the optical measurement setup. An in-plane external magnetic field H_{DC} is applied in the direction of the angle θ from the x-axis. As in the electrical transmission measurements, the spin waves are excited by applying microwaves to the microstrip antenna connected to Port 1 of the VNA, and the excited spin wave propagates in the $\pm k$ directions, which correspond to the $\pm x$ directions, respectively. From the z-direction, a linearly polarized laser beam with a wavelength of 660 nm is input and focused on the surface of the thin magnetic film where the spin waves are excited. The optical spot diameter is about 2 μm. The polarization of the light reflected from the thin film surface, where the spin waves exist, rotates at the spin wave frequency due to the polar Kerr effect. This dynamic rotation is converted into dynamic intensity modulation by passing through a half-wave plate and a polarizing beam splitter, which is electrically detected at Port 2 of the VNA via a photodiode.

The transmission coefficient $S_{21,\pm k}$ is obtained at each optical spot position x for the spin waves in the $\pm k$ directions. The antenna position is $x = 0$, as shown in Fig. 2(a). The output power from the VNA is set to -5 dBm, the frequency range is 8.5 to 18 GHz in 11.5 MHz steps, and the IF bandwidth is set to 100 Hz. We use the device shown in Fig. 2(a) for optical imaging measurements, which has a different antenna separation distance of 25 μm from the device for the electrical transmission measurements shown in Fig. 1(a). All other designs are the same. The reason for increasing the antenna separation distance is to suppress the effect of the spin waves propagating in the $-k$ direction being reflected by the other antenna.

Figure 2(b) shows the distance $|x|$ dependence of the sum of the transmission coefficient amplitude $\sum_{\omega_a(|k|=0)}^{\omega_a(|k|=1\,\mu\mathrm{m}^{-1})} |S_{21,\pm k}|$ under $\theta = 90$ degrees and $\mu_0 H_{\mathrm{DC}} = 50$ mT. The black lines show the fitting results using $A_{\pm k} e^{-x/\lambda_{\pm k}}$. The red and blue plots in the upper and lower panels of Fig. 2(c) show the magnetic field angle dependence of the fitting parameters: the amplitude $A_{\pm k}$ and propagation length $\lambda_{\pm k}$. Note that the results for angles of less than 30 degrees are not obtained because preliminary experiments confirm that the spin wave excitation efficiency is low and the signal-to-noise ratio of the optical measurement is low. Figure 2(d) shows the angular dependence of the ratio $R_A = A_{+k}/A_{-k}$ and $R_\lambda = \exp\left(-\frac{10\,\mu\mathrm{m}}{\lambda_{+k}}\right) / \exp\left(-\frac{10\,\mu\mathrm{m}}{\lambda_{-k}}\right)$, obtained from the amplitude and propagation length obtained by the fitting. We use $|x| = 10$ μm for R_λ calculation to study spin wave propagation in the device with a 10 μm distance between the antennas, which is used in the electrical measurement. The upper panel of Fig. 2(d) shows that R_A and the theoretical value κ_t agree quantitatively. From the lower panel, R_λ is not always 1, increasing at $\theta = 30$ degrees. These results indicate that the propagation length is not symmetrical. As Fig.

2(e) shows, the angular dependence of the nonreciprocity κ_e from the electrical measurement is not reproduced by the theoretical value κ_t, represented as white lines in Figs. 1(c) and 1(d), respectively. However, the angular dependence of $\kappa' = R_A \times R_\lambda$, including the propagation length asymmetry, is consistent with that of κ_e above 30 degrees . The results demonstrate that the nonreciprocity κ_e around 30 degrees is due to the asymmetry of the propagation length. For the origin of the nonreciprocity, it is essential to consider the contributions of both the asymmetries of the excitation efficiency and the propagation length.

Possible mechanisms of the asymmetry of the spin wave propagation length are the following: the asymmetry of the dissipation of the spin wave energy to other physical systems due to the spin pumping [10),11)] or the phonon-magnon coupling [12)-14)] and the asymmetry of the dispersion relation due to the Dzyaloshinskii-Moriya interaction (DMI) [15),16)]. Further investigation is required to discuss the relationship between our results and these effects.

Comparing κ' and κ_e at magnetic field angles of less than 30 degrees is important for discussing the origin of the observed nonreciprocity in more detail. For this purpose, the future outlook is to improve the signal-to-noise ratio of optical measurements by making spin wave excitation antennas more efficient and enhancing optical signals.

3. Conclusion

In this study, we investigate the angular dependence of the nonreciprocity of the spin wave in the magnetic thin film using electrical transmission measurements. We find that the existence of nonreciprocity that cannot be explained by the previously known asymmetry of the spin wave excitation efficiency. By performing optical imaging, we confirm that the nonreciprocity is due to the direction-dependent spin wave propagation length. Results obtained in this study will be helpful for future research on information transport devices using spin waves.

Acknowledgements This work was supported by JSPS KAKENHI (grant no. JP21K18145, JP22K14589, JP22KJ1995, JP23KJ1209, JP23KJ1159, JP24H00007, JP24H02233), JST (grant no. JPMJFS2123, JPMJPR200A), MEXT Initiative to Establish Next-generation Novel Integrated Circuits Centers (X-NICS) (grant no. JPJ011438), and the Collaborative Research Program of the Institute for Chemical Research, Kyoto University.

References

1) K. Sekiguchi, K. Yamada, S. M. Seo, K.-J. Lee, D. Chiba, K. Kobayashi, and T. Ono: *Appl. Phys. Lett.*, **97**, 022508 (2010).
2) M. Jamali, J. H. Kwon, S. M. Seo, K. J. Lee, and H. Yang: *Sci. Rep.*, **3**, 3160 (2013).
3) J. Chen, H. Yu, and G. Gubbiotti: *J. Phys. D Appl. Phys.*, **55**, 123001 (2022).
4) B. Flebus, D. Grundler, B. Rana, Y. Otani, I. Barsukov, A. Barman, G. Gubbiotti, P. Landeros, J. Akerman, U. S. Ebels, P. Pirro, V. E. Demidov, K. Schultheiss, G. Csaba, Q. Wang, D. E. Nikonov, F. Ciubotaru, P. Che, R. hertel, T. Ono, D. Afanasiev, J. H. Mentink, T. Rasing, B. Hillebrands, S. Viola Kusminskiy, W. Zhang, C. R. Du, A. Finco, T. van der Sar, Y. K. Luo, Y. Shiota, J. Sklenar, T. Yu, and J. Rao: *J. Phys.: Condens. Matter*, **36**, 363501 (2024).
5) T. Schneider, A. A. Serga, T. Neumann, B. Hillebrands, and M. P. Kostylev, *Phys. Rev. B*, **77**, 214411 (2008).
6) M. Nakayama, K. Yamanoi, S. Kasai, S. Mitani, and T. Manago: *Jpn. J. Appl. Phys.*, **54**, 083002 (2015).
7) B. A. Kalinikos and A. N. Slavin: *J. Phys. C: Solid State Phys.*, **19**, 7013 (1986).
8) Y. Shiota, S. Funada, R. Hisatomi, T. Moriyama, and T. Ono: *Appl. Phys. Lett.*, **116**, 192411 (2020).
9) Y. Shiota, R. Hisatomi, T. Moriyama, and T. Ono: *Phys. Rev. B*, **102**, 214440 (2020).
10) S. Mizukami, Y. Ando, and T. Miyazaki: *Phys. Rev. B*, **66**, 104413 (2002).
11) J. H. Kwon, J. Yoon, P. Deorani, J. M. Lee, J. Sinha, K. -J. Lee, M. Hayashi, and H. Yang: *Sci. Adv.*, **2**, e1501892 (2016).
12) R. Sasaki, Y. Nii, Y. Iguchi, and Y. Onose: *Phys. Rev. B*, **95**, 020407 (2017).
13) S. Streib, H. Keshtgar, and G. E. W. Bauer: *Phys. Rev. Lett.*, **121**, 027202 (2018).
14) R. Schlitz, L. Siegl, T. Sato, W. Yu, G. E. W. Bauer, H. Huebl, and S. T. B. Goennenwein: *Phys. Rev. B*, **106**, 014407 (2022).
15) F. Garcia-Sanchez, P. Borys, A. Vansteenkiste, J. Kim, and R. L. Stamps: *Phys. Rev. B*, **89**, 224408 (2014).
16) M. Kuepferling, A. Casiraghi, G. Soares, G. Durin, F. Garcia-Sanchez, L. Chen, C. H. Back, C. H. Marrows, S. Tacchi, and G. Carlotti: *Rev. Mod. Phys.*, **95**, 015003 (2023).

Received Oct. 23, 2024; Accepted Nov. 15, 2024